Optics, Acoustics, and Stress in a Nearshore Bottom Nepheloid Layer

Paul S. Hill
Department of Oceanography
Dalhousie University
Halifax, Nova Scotia, CANADA B3H 4J1
phone: (902) 494-2266 fax: (902) 494-3877 email: paul.hill@dal.ca

Timothy G. Milligan
Fisheries and Oceans Canada
Bedford Institute of Oceanography
1 Challenger Drive
Dartmouth, Nova Scotia, CANADA B2Y 4A2
phone: (902) 426-3273 fax: (902) 426-6695 email: milligant@mar.dfo-mpo.gc.ca

Grant Numbers: N000140410278 and N000140410233
http://www.phys.ocean.dal.ca/~phill

LONG-TERM GOALS

The goal of this research is to develop greater understanding of the how the flocculation of fine-grained sediment responds to turbulent stresses and how this packaging of sediment affects optical and acoustical properties in the water column.

OBJECTIVES

1. Quantify the effects of aggregation dynamics on the size distribution of particles in the bottom boundary layer;
2. Quantify how changes in particle packaging affect the optical and acoustical properties of the water column.
3. Develop models describing the associations between particle aggregation, stress, and the acoustical and optical fields.

APPROACH

The approach is to obtain measurements that will permit comparisons of temporal evolution of bottom stress, suspended particle size, and optical and acoustical properties in the bottom boundary layer. The instrumentation is mounted on bottom tripods and an I-beam frame. The “OASIS” tripod includes a 9-wavelength optical attenuation and absorption meter (WetLabs ac-9, with automated dissolved measurement for calibration-independent particulate measurements), LISST-100 (Type B) and LISST-Floc laser diffraction particle sizers (Agrawal & Pottsmith 2000), a digital floc camera (DFC) (Curran et al. 2002), a Tracor Acoustic Profiling System (TAPS) (Holliday 1987), and an array of SonTek/YSI acoustic Doppler velocimeters (ADVs). Near-simultaneous ac-9 measurements with and without a filter assure high-quality particulate spectral absorption and attenuation measurements. The LISSTs and DFC together provide particle size distributions from 1.25 µm to 1 cm in diameter. The TAPS and ADVs obtain acoustical backscatter intensity over a wide range of frequencies that can be used to

Report Documentation Page

Form Approved
OMB No. 0704-0188

1. REPORT DATE **2008**	2. REPORT TYPE	3. DATES COVERED **00-00-2008 to 00-00-2008**
4. TITLE AND SUBTITLE **Optics, Acoustics, and Stress in a Nearshore Bottom Nepheloid Layer**		5a. CONTRACT NUMBER 5b. GRANT NUMBER 5c. PROGRAM ELEMENT NUMBER
6. AUTHOR(S)		5d. PROJECT NUMBER 5e. TASK NUMBER 5f. WORK UNIT NUMBER
7. PERFORMING ORGANIZATION NAME(S) AND ADDRESS(ES) **Dalhousie University,Department of Oceanography,Halifax, Nova Scotia, CANADA B3H 4J1,**		8. PERFORMING ORGANIZATION REPORT NUMBER
9. SPONSORING/MONITORING AGENCY NAME(S) AND ADDRESS(ES)		10. SPONSOR/MONITOR'S ACRONYM(S) 11. SPONSOR/MONITOR'S REPORT NUMBER(S)
12. DISTRIBUTION/AVAILABILITY STATEMENT **Approved for public release; distribution unlimited**		
13. SUPPLEMENTARY NOTES		
14. ABSTRACT		
15. SUBJECT TERMS		

16. SECURITY CLASSIFICATION OF:			17. LIMITATION OF ABSTRACT	18. NUMBER OF PAGES	19a. NAME OF RESPONSIBLE PERSON
a. REPORT **unclassified**	b. ABSTRACT **unclassified**	c. THIS PAGE **unclassified**	**Same as Report (SAR)**	**8**	

generate particle size distributions (Holliday, 1987; Hay and Sheng, 1992). In 2006-2007 a new tripod was constructed and deployed. It is called the Modified In Situ Size and Settling Column Tripod (MINSSECT). It was developed to provide better constraint on conversions between optical signals, particle area, and particle mass. It carries a digital floc camera, a LISST-100 (Type B), a video settling column, and an automated water transfer system. The equipment on this tripod monitors in situ particle size distribution from 1.25 µm to 1 cm in diameter and size versus settling velocity for particles larger than approximately 100 µm. The water transfer system provides direct estimates of the mass in suspension that can be used to calibrate the beam attenuation coefficient to suspended mass. The I beam array consists of 4 of SonTek/YSI acoustic Doppler velocimeters (ADVs) mounted vertically ~ 0.25 m above the bottom.

The combined optical and acoustical measurements provide a comprehensive description of the suspended particles near the seabed. The velocity measurements obtained from the I-beam-mounted ADVs provide direct-covariance estimates of Reynolds stress and inertial-range estimates of the dissipation rate for turbulent kinetic energy (Shaw and Trowbridge, 2001).

Hill and Milligan collaborate closely on this project. Together they are providing data and models on the flocculated size distribution of suspended sediment. Milligan and Hill have responsibility for the DFC on the OASIS tripod and for the entire MINSSECT. Brent Law (BIO), Kristian Curran (Dal) and John Newgard (Curran's replacement) provide support in the lab and field.

We also collaborate with Emmanuel Boss (UMaine) and John Trowbridge (WHOI) on this project. Boss is responsible for all optical and acoustical characterization of the water column. He has also conducted laboratory manipulations of the particle size distribution in order to explore the effect on optical attenuation. Boss and Hill have worked together on an optical model of marine aggregates. John Trowbridge is responsible for characterizing the stress in the bottom boundary layer during the deployments. We also collaborate with Oscar Schofield (Rutgers) who deployed gliders in the study area during our September 2007 deployment. A group from WetLabs deployed a profiling mooring during part of our September 2007 deployment. Yogi Agrawal (Sequoia Scientific) placed a prototype "LISST Back" on MINSSECT for part of our September 2007 deployment.

WORK COMPLETED

Work was completed in three areas during 2007. First, analysis of data from a 2005 deployment was completed. Second, a model for floc size and floc fraction was developed and compared with the 2005 data. Finally, analysis of 2007 data was completed, with some issues still under investigation.

The analysis of 2005 data is complete. The responses of floc size and floc packaging to shear stress have been characterized (Fig. 1).

A model of floc size and floc fraction is under development (Figs. 2 and 3). It follows the strategy of Winterwerp (e.g. Winterwerp et al., 2006) in assuming that the equilibrium floc size in a suspension is determined by a balance between aggregation, disaggregation, and settling. The settling component has not been implemented yet.

Data from the 2007 deployment have been worked up. Merged size distributions have be generated. Size-settling velocity relationships for large flocs have been estimated, and disaggregated inorganic size distributions as well as suspended particulate mass (SPM) concentrations have been measured from in-situ filtered samples. All of these measurements have been compared to particulate attenuation and boundary shear stress.

Our steady, 1-D model of optical attenuation in continental-shelf bottom boundary layers awaits the implementation of the floc model described above and of a method for correcting for the effect of suspended sediment stratification. The model is an adaptation of Pat Wiberg's successful model (Wiberg et al., 1994).

RESULTS

For the 2005 data floc fraction was estimated by summing the particle areas in the sizes greater than 133 μm (cf. Mikkelsen et al., 2006) and dividing by the total area in the merged particle size distribution. This proxy for mass fraction is justified because for marine aggregates, particle area and particle mass scale similarly with diameter (refer to Boss annual report). Maximum floc size was equated with the size at which cumulative particle area in a distribution reached 95% of the total. Spectral absorption and attenuation were measured with an ac-9, and the ratio of absorption at 676 nm to attenuation at 555 nm was used as a proxy for the composition of suspended matter. A high value indicates a suspension rich in chlorophyll containing particles, and a low value indicates that non-pigmented particles dominate the suspension. All particle size spectra were sorted into groups of similarly shaped spectra using entropy analysis.

Plots of maximum floc size and floc fraction versus shear velocity and total suspended area are wedge-shaped (Figure 1). At low shear velocities, floc size and floc fraction extend across a wide range of values. As shear velocity increases, the upper limits of floc size and floc fraction decrease. At high shear velocity, floc size and floc fraction are small and do not vary greatly. Similar patterns describe the relationships of floc size and floc fraction to area. Both have large ranges with large upper limits when suspended area is low. These upper limits decrease as area increases. The spectral optical properties suggest that rising shear velocities and areas are associated with a compositional change in the suspension. The suspension contains relatively less pigmented particles when shear velocity and area are high. This pattern is caused by the resuspension of inorganic material from the bed as shear velocity rises.

Plots of modeled maximum floc size and floc fraction as functions of turbulence and sediment concentration show two basic behaviors (Figures 2 and 3). Turbulence is represented by shear velocity in the figures. Floc fraction depends on sediment concentration and turbulence. It is highest when sediment concentration is high and turbulence is weak. It falls to zero as concentration decreases and as turbulence increases. In contrast, maximum floc size is determined almost entirely by turbulence. This prediction differs from those of other models that predict that maximal floc size should increase with increasing concentration (e.g., Winterwerp et al., 2006). The validity of these predicted trends in floc size and floc fraction can be assessed with the data.

The upper surface of the wedge of data in the plot of maximum floc size versus shear velocity is consistent with model predictions. As turbulence increases, floc size decreases. According to the model, the large range of values at low shear velocities cannot be caused by variable concentration. Instead it must reflect compositional variability. This prediction is also consistent with the data, which show a clear shift in optical composition as shear velocity rises. Likewise, the upper surface of the wedge of data in the plot of floc fraction versus shear velocity is consistent with model predictions. In the model, turbulence is the dominant control on floc fraction except at very low concentrations. The spread of values at a given shear velocity also likely arises from compositional variability.

At first glance, the trends in floc size and floc fraction with suspended area are not consistent with model predictions. The upper surfaces of the data wedges in the plots of floc size and floc fraction versus area decrease with increasing area. The model, however, predicts that floc size does not depend on sediment concentration and that floc fraction, at least at low concentrations, should increase with increasing concentration. Model and data can be reconciled by recognizing that concentration and turbulence are not independent in bottom boundary layers. As turbulence increases, resuspension of sediment from the seabed increases concentration. In fact, concentration increases approximately as the square of shear velocity. As a result, large concentrations are associated with large shear velocities. Large shear velocities are associated with small floc size and floc fraction. The wedge shape of the plots reflects the overriding control of turbulence on floc size and floc fraction. Again, the large range in floc size and floc fraction at small areas likely reflects compositional variability.

The 2007 SPM data have allowed us to explore the accuracy of sediment area concentrations estimated by the LISST and the DFC. These instruments can give estimates of area concentration that differ by an order of magnitude, yet there is uncertainty regarding which is more accurate. In theory, if suspended particles are large relative to the wavelength of light, then twice the summed area should be approximately equal to the particulate attenuation as measured by the LISST (Figure 4). Summed camera areas are too low to explain observed attenuation because the camera does not resolve particles smaller than about 60 μm. Summed LISST areas, in contrast, greatly exceed expectations, suggesting some problem in conversion of scattered light intensity to particle area concentration for natural suspended particles. Merged size distributions, generated by correcting LISST concentrations downward to match DFC concentrations in the region of overlap, are of the proper magnitude to explain observed attenuations. This finding suggests that the DFC is more accurate for estimating suspended particle concentration.

IMPACT/APPLICATIONS

The high resolution time series of particle, optical, and acoustical properties will enhance understanding of the rates and mechanisms by which the water column clears following storm events. Development of a 1-D model includes the development of a floc module and a module that converts sediment to optical properties. The latter advance will provide the sedimentology community with a simple tool to test their model predictions against the most ubiquitous measurement of suspended matter in coastal waters.

RELATED PROJECTS

Hill has a project funded by NSERC (Canada) that investigates the effect of in situ particle size distribution on the interaction of oil and sediment in suspension. This project funded the purchase of the LISST-100 on the MINSSECT.

REFERENCES

Agrawal, Y. C., Pottsmith, H.C. 2000. Instruments for particle size and settling velocity observations in sediment transport. Marine Geology, 168: 89-114.

Curran, K.J., Hill, P.S, Milligan, T.G. 2002. Fine-grained suspended sediment dynamics in the Eel River flood plume. Continental Shelf Research, 22: 2537-2550.

Hay, A.E., Sheng, J. 1992. Vertical profiles of suspended sand concentration and size from multifrequency acoustic backscatter. Journal of Geophysical Research (Oceans), 97: 15661-1567.

Holliday, D.V. 1987. Acoustic determination of suspended particle size spectra. IN Proceedings of a Specialty Conference on Advances in Understanding of Coastal Sediment Process, Coastal Sediments - 1987, 1: 260-272.

Mikkelsen, O.A., Hill, P.S., Milligan, T.G. 2006. Single-grain, microfloc and macrofloc volume variations observed with a LISST-100 and digital floc camera. Journal of Sea Research, 55: 87-102.

Shaw, W.J., Trowbridge, J.H. 2001. The direct estimation of near-bottom turbulent fluxes in the presence of energetic wave motions. Journal of Atmospheric and Oceanic Technology, 18: 1540-1557.

Wiberg, P. L., Drake, D. E. and Cacchione, D. A. 1994. Sediment resuspension and bed armoring during high bottom stress events on the northern California inner continental shelf: Measurements and predictions. Continental Shelf Research, 14: 1191-1220.

Winterwerp, J. C., A. J. Manning, C. Martens, T. de Mulder and J. Vanlede, 2006. A heuristic formula for turbulence-induced flocculation of cohesive sediment. Estuarine, Coastal and Shelf Science, 68: 195-207.

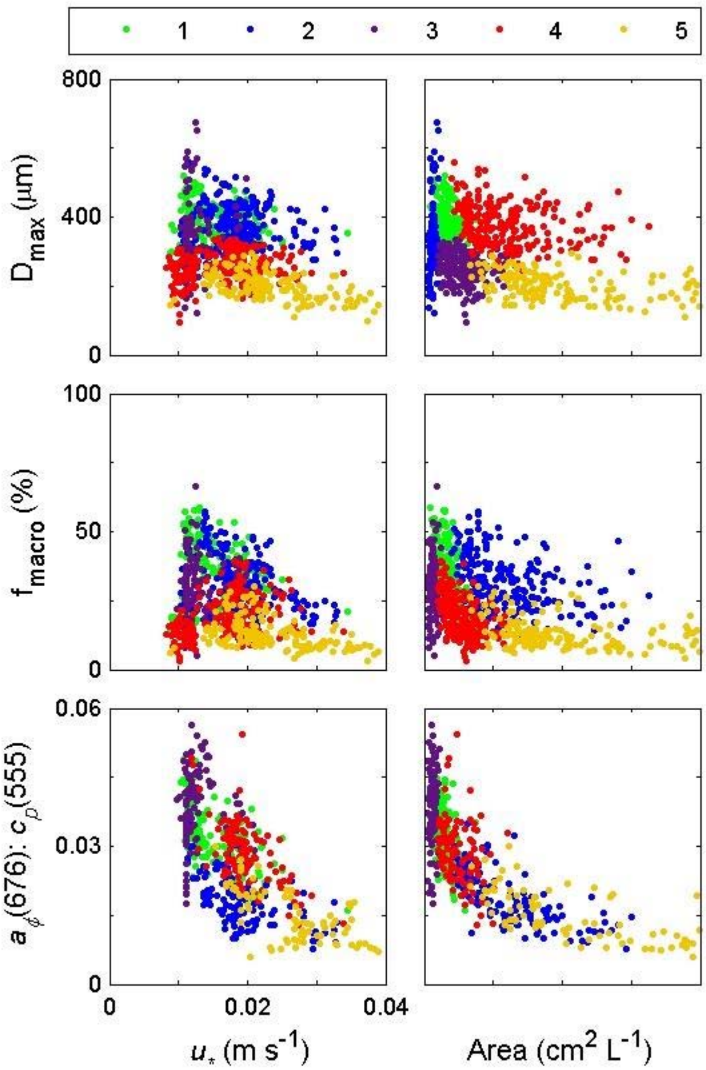

Figure 1. Maximum floc size (D_{max}) (top row), floc fraction (f_{macro}) (middle row), and the ratio $a_\Phi(676)\ c_p(555)^{-1}$ (bottom row) versus combined wave-current turbulent shear velocity (u_*) (left column) and area concentration in suspension (right column). The ratio $a_\Phi(676)\ c_p(555)^{-1}$ is a relative measure of the amount of pigmented particles to total particles in suspension. Different colors denote the 5 entropy groups, which contain statistically similar size distributions. Plots of maximum floc size versus shear velocity and suspended area are wedge-shaped, with a large spread of floc sizes at small shear velocities and suspended areas. The distributions of values of maximum floc size taper to small spreads at larger shear velocities and suspended area concentrations. The taper arises from a reduction in the upper limit of observed sizes. The largest observed floc sizes are about 600 micrometers. At high stresses and areas, this upper limit decreases to about 200 micrometers. This same pattern holds for floc fraction. At low shear velocities and suspended areas, floc fraction ranges from 0.1 to 0.75. At high shear velocities and suspended areas, floc fractions are all around 0.1. The optical ratio shows more of a hyperbolic distribution, decreasing from high values of around 0.06 at low shear velocities and suspended areas to low values of around 0.01 for higher shear velocities and areas.

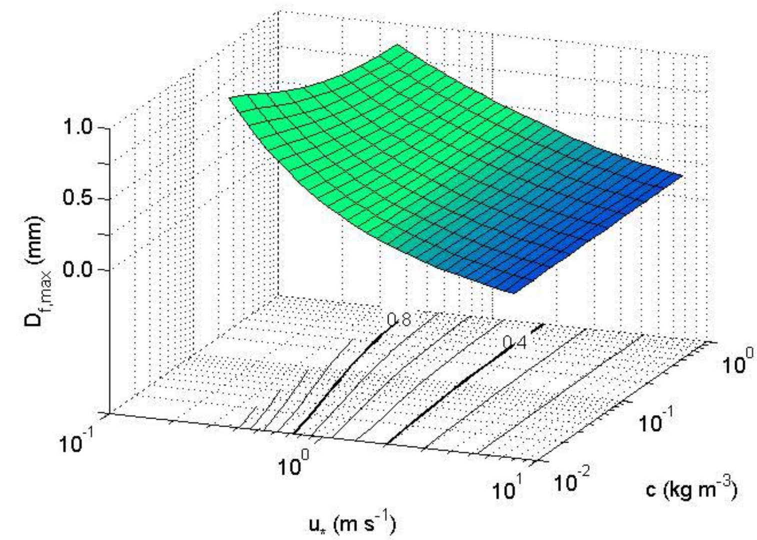

Figure 2. Predicted response of equilibrium maximum floc size to changes in shear velocity and sediment concentration. The 3-D shaded surface shows that floc size responds primarily to shear velocity and has little dependence on sediment concentration. Contours of floc size below the shaded surface plot floc size in shear velocity/concentration space. When shear velocity is below 1 cm s^{-1}, floc size approaches 1 mm with the model inputs used here. As shear velocity increases to 10 cm s^{-1}, floc size decreases to several hundred micrometers. At these higher shear velocities, floc size does not depend on sediment concentration.

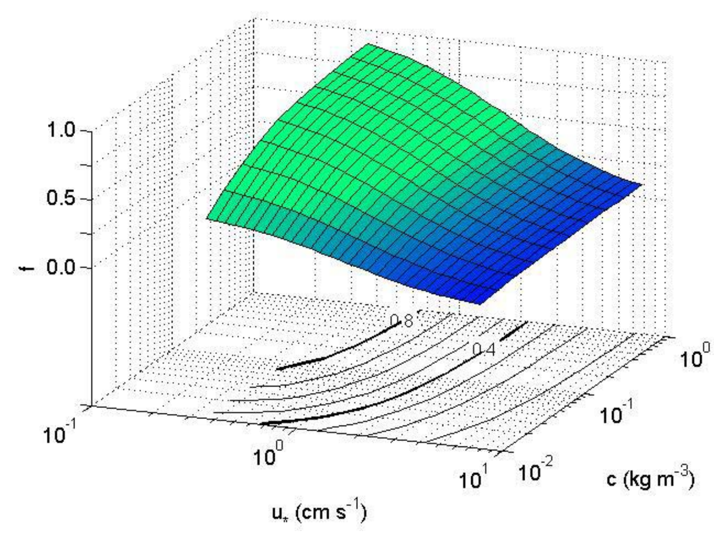

Figure 3. Predicted response of equilibrium floc fraction to changes in shear velocity and sediment concentration. The 3-D shaded surface shows that floc fraction responds primarily to shear velocity when sediment concentration is large. At low sediment concentrations, floc fraction is reduced. Contours of floc fraction below the shaded surface portray these relationships in shear velocity/concentration space. When shear velocity is below 1 cm s^{-1}, floc fraction ranges from 0.4 at low concentration to 0.8 at high concentration. As shear velocity increases to 10 cm s^{-1}, floc fraction is near zero for all sediment concentrations.

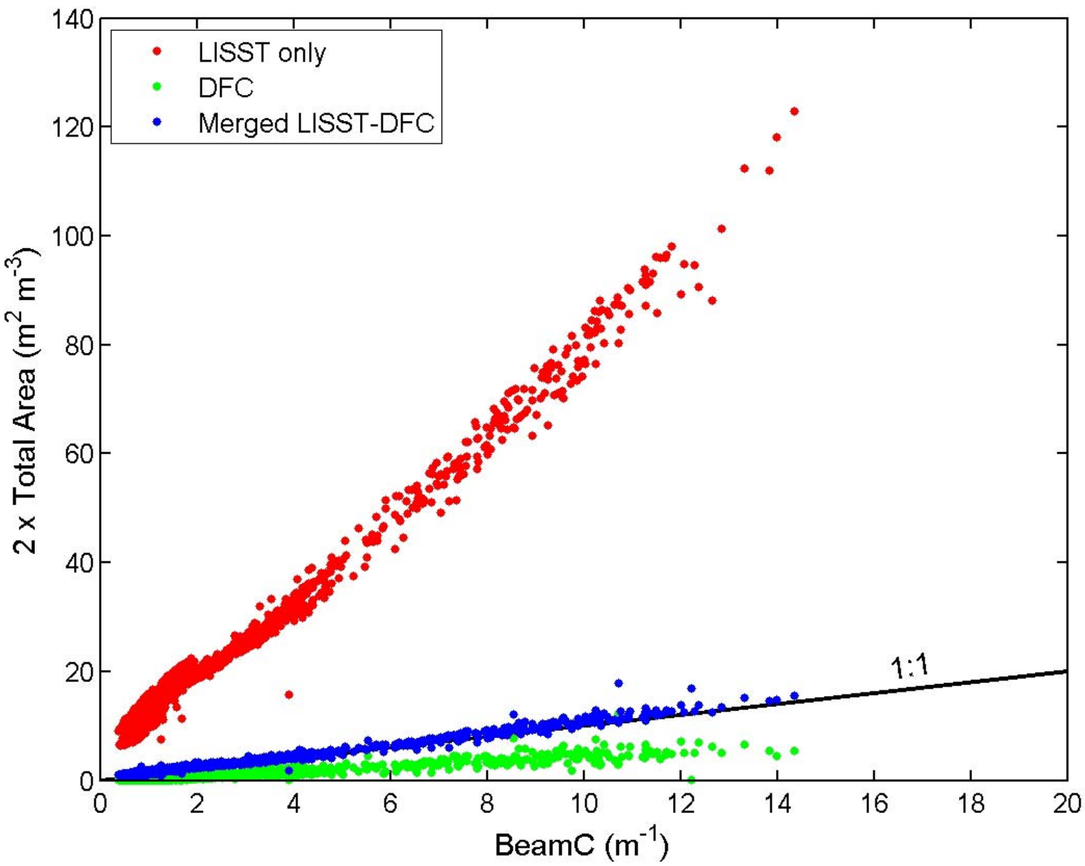

Figure 4. Plot of 2 times the suspended particle projected area measured 3 ways on the y axis versus the attenuation coefficient on the x axis. Also shown is a 1:1 line. Theoretically, if the particles are much larger than the wavelength of light, then the data should plot along the 1:1 line. When suspended area is estimated from the DFC, the data plot below the 1:1 line, indicating that the DFC alone underestimates the total suspended area concentration. This result arises because the camera does not resolve particles smaller than 60 μm. When suspended area is estimated from the LISST, which resolves particles between 1.25 and 250 μm, the data plot well above the 1:1 line. In fact, a regression through the data (not shown) has a slope of approximately 10:1, indicating that the LISST is over-estimating suspended area concentration by a factor of 10. The causes of this over-estimation are under investigation. Finally, the data fall close to a 1:1 line if suspended area is estimated from merged size distributions, which are calculated by correcting the LISST concentrations so that they match the DFC concentrations in the region of overlap. This result suggests that the DFC produces more accurate estimates of suspended area concentration.